NMR and Entangled Chain Dynamics in Molten Polybutadiene. Molecular Weight Dependent Segmental Friction

Jean-Pierre Cohen Addad* and Armel Guillermo

Laboratoire de Spectrométrie Physique, associé au CNRS (UMR C5588) Université Joseph Fourier, Grenoble I. B.P. 87 - 38402, St Martin d'Hères Cedex, France

Received October 8, 2002

ABSTRACT: The chain dynamics in high molecular weight polymer melts observed from proton magnetic relaxation generates a reference frequency, $\Delta \approx 10^3$ rad·s^{-1}, closely related to the chain entanglement interaction. Observing polybutadiene, we report on the slight molecular weight dependence of the segmental correlation time τ_s^I associated with the time scale $1/\Delta \approx 10^{-3}$ s, ($41 \times 10^3 \leq M \leq 375 \times 10^3$); τ_s^I is shown to exhibit an apparent power law $M^{0.31}$. Correspondingly, the reptation time is expected to go as $M^{3+(0.31\pm0.03)}$ within the intermediate range $41 \times 10^3 \leq M \leq 375 \times 10^3$. This semilocal property and the chain self-diffusion $M^{-\beta}$ ($\beta = 2.3 \pm 0.1$ instead of 2) dependence, recently reported for many polymers and solutions, suggest a chain dynamics governed by a semilocal friction effect varying as an apparent $M^{0.3}$ power law instead of M^0. A thorough analysis of the pattern of proton relaxation curves is proposed; end-submolecules (≈60 monomeric units) are distinguished from inner ones from their magnetization dynamics; these are described as nonexponential time functions in accordance with the observation of pseudo-solid echoes (PSOSES). The molecular weight dependent pattern of four species of curves (two relaxation types and two PSOSE types) corresponding to 40 recorded curves is quantitatively analyzed using only four independent adjustable parameters.

1. Introduction

For a polymer melt formed from long chains of mass M, the power law currently observed for the zero-shear rate viscosity is $M^{3.4}$ while according to the reptation theory, the terminal relaxation time of the dynamics of one chain, T_r, is predicted to vary as M^3.[1,2] This dependence is based on the assumption that the monomeric friction coefficient is molecular weight independent; correspondingly, the curvilinear diffusion coefficient of one chain during its back and forth reptational movement varies as M^{-1}. The discrepancy in the exponent of the viscosity has been a matter of debate which is not yet settled. Curtiss and Bird suggested that the segmental friction coefficient may depend on the chain molecular weight M^3. This hypothesis was considered for many years as contradicting results of self-diffusion experiments; however, the thorough analysis of data recently reported by Lodge and by Tao et al. and our own recent results about polybutadiene (PB) have shown that the self-diffusion coefficient actually varies as $M^{-\beta}$ with $\beta = 2.28 \pm 0.05$ or 2.4 ± 0.1 instead of M^{-2}.[4−6] Furthermore, the crossover between the Rouse behavior of the self-diffusion process (M^{-1} dependence) and the reptation behavior ($M^{-2.4}$ dependence) was precisely shown to occur for a molecular weight $M_D = 31.7 \times 10^3$ for PB. These experimental results suggest that the friction coefficient involved in long-range chain dynamics may depend on M according to the power law M^α with $0.3 \leq \alpha \leq 0.4$. Moreover, most recent numerical simulations about reptation dynamics have given evidence for a transient regime for the molecular dependence of the terminal relaxation time, T_r; in this regime, it should vary as $M^{3.3}$ while the M^3 dependence should occur for very long chains only.[7,8]

The purpose of this work was to give evidence for the slight molecular weight dependence of a segmental friction effect introduced in the analysis of NMR properties.

For systems of long linear chains, the viscoelastic relaxation spectrum exhibits two well-defined dispersions: the transition domain at short times and the terminal domain at long times. The transition dispersion is insensitive to chain length and associated with local chain motions. The terminal dispersion is associated with large scale rearrangements of chain conformation that are described according to the reptation model. The two dispersions are well-separated, resulting in a rubberlike plateau response at intermediate times or frequencies; it may be considered that there is a break in the dynamic fluctuations that occur along one chain. The plateau property is one of the characteristics of molten polymers that have been attributed to chain entanglement interactions.[9,10]

Correspondingly, the motional averaging process of dipole−dipole interactions of protons attached to long linear chains in a melt occurs according to two steps reflected by the transverse magnetic relaxation. During the first step, nonisotropic local chain motions associated with the transition dispersion induce a partial averaging process of proton dipolar interactions; the resulting partial average called Δ (≈10^3 rad·s^{-1}) is closely related to the break in the dynamics of fluctuations. This NMR property reflects the rubberlike plateau response characterized by the modulus G_N^0. One of the main features about the NMR approach to polymer dynamics is that the chain entanglement interaction generates the residual dipole−dipole coupling Δ which may serve as a low-frequency reference independent of chain molecular weight.

The second step of the motional averaging process applies to the residual proton−proton coupling and corresponds to the terminal dispersion; however, the analysis of the effect of large scale rearrangements on

10.1021/ma021567y CCC: $25.00
Published on Web 02/06/2003

NMR requires the terminal domain be more precisely described: considering the model proposed by De Gennes, rearrangements are supposed to occur according to two dynamics steps. The first one, also called equilibration process, is usually described from the Rouse model while the second step corresponds to the chain reptation. Because chain reptation is too slow, it does not contribute to the motional averaging of the proton dipole−dipole interactions.

Another characteristic property of molten polymers is the molecular weight M_c, governing the behavior of zero-shear rate viscosity η_0; it separates the short chain dependence ($\eta_0 \alpha M$) and long chain dependence ($\eta_0 \alpha M^{3.4}$). This property implies the existence of a characteristic segment originating from the chain entanglement interaction; its molecular weight is usually defined as $M_e = \rho RT/G_N^o$ (ρ is the polymer density). The transition dispersion reflects the spectrum of fluctuations which occur within this characteristic segment defined from about 50 monomeric units in polybutadiene; it is considered that these segmental fluctuations are also involved in the determination of the partial average of dipole−dipole interactions, Δ. The residual dipole−dipole coupling is also observed in permanent networks; in these systems, it is associated with the mean segmental size between two junction loci which correspond to breaks in the dynamic fluctuations, too.

In this work, proton relaxation properties specific to a melt were carefully observed from molten polybutadiene ($41 \times 10^3 \leq M \leq 375 \times 10^3$). The analysis of transverse relaxation curves started from NMR studies recently reported about poly(ethylene-oxide) (PEO) and polybutadiene;[6,11−13] considering one linear chain comprised of N monomeric units, these studies have shown that the normalized relaxation function $M_x^T(t,N)$ consists of several well-distinguished contributions:

$$M_x^T(t,N) = M_x^I(t,N)\Phi_R^I(t) + M_x^{II}(t,N)\Phi_R^{II}(t) \qquad (1)$$

already observed on other polymers,[14,15] $M_x^{II}(t,N)\Phi_R^{II}(t)$ has been associated with protons attached to so-called end-submolecules formed from about 60 monomeric units in polybutadiene while $M_x^I(t,N)\Phi_R^I(t)$ has been assigned to protons attached to the remaining part of the chain;[13] this contribution has been supposed to be governed both by residual dipole−dipole coupling and by the dynamics of large scale chain fluctuations. $\Phi_R^{II}(t)$ and $\Phi_R^I(t)$ have been assigned to the relaxation contributions induced by fast random motions of monomeric units forming either end-submolecules or the remaining part of one chain, respectively; they were not distinguished from each other in previous works. $M_x^I(t,N)$ and $M_x^{II}(t,N)$ are chain length dependent and can be determined independently of $\Phi_R^I(t)$ and $\Phi_R^{II}(t)$, as reported elsewhere.[13,16]

Ignoring the slow reptation motion, the description of $M_x^I(t,N)$ has been based on the Rouse model extended to NMR. The segmental friction introduced in this model is usually considered as molecular weight independent; in this work, it will be shown that it varies according to a power law characterized by a small exponent. However, the determination of the low exponent value ($\approx$0.3) requires experimental results be carefully analyzed; consequently, this work consisted of two parts. To begin with, it was essential to prove that the theoretical NMR approach was fully appropriate to the understanding of the proton relaxation; the validity of the proposed description of the relaxation function was checked by observing several characteristic properties predicted from the model, including properties of so-called pseudo-solid spin echoes (PSOSES), which reflect a time reversal effect specific to the existence of residual dipole−dipole couplings. Then, relaxation curves were rigorously analyzed to give a reliable evidence for the molecular weight dependence of the segmental friction effect. In addition to the description of this property, this work provides a quantitative analysis of proton transverse relaxation and PSOSES; attention was focused on the $M_x^{II}(t,N)$ relaxation roughly represented as an exponential time function in previously reported studies, ignoring the observation and the analysis of PSOSES specific to this contribution.

2. Experimental Section

Polybutadiene samples (polydispersity: $1.03 \leq I_p \leq 1.07$) were bought from Polymer Source Inc. (Canada); the chain microstructure was around 68% *cis*-1,4-, 27% *trans*-1,4- and 5% 1,2-vinyl. Proton relaxation curves were recorded using a Bruker MSL 300 spectrometer operating at 60 MHz. All samples were kept in tubes sealed under vacuum; the sample temperature was controlled within ±1 K. Relaxation curves were obtained by forming Hahn spin echoes (pulse sequence, $90°/x-\tau-[180°/x-2\tau-180°/-x-2\tau-180°/-x-2\tau-180°/x-2\tau-]_n$); so-called pseudo-solid spin echoes specific to the existence of a nonzero average of dipole−dipole interactions were formed by applying the following pulse sequence to the spin-system: $90°/x-\tau-180°/x-\tau-90°/y-\tau_1-[180°/x-2\tau_1-180°/-x-2\tau_1-180°/-x-2\tau_1-180°/x-2\tau_1-]_n$.[11]

3. NMR Theoretical Basis

It is not the purpose of this paper to recall the whole theoretical NMR background underlying this work. The analysis of the proton transverse relaxation in entangled polymers relies on the assumption that the dynamics of one chain can be described in terms of the motions of submolecules; the physical origin of submolecules is qualitatively associated with the effect of temporary elasticity, i.e., a break in chain dynamics fluctuations.[16] Considering that the motions of monomeric units forming end-submolecules of one chain are less anisotropic than those of monomeric forming the remaining submolecules, the relaxation curve consists of two parts (I and II) represented by two relaxation functions governed by two different residual dipole−dipole couplings called Δ_I and Δ_{II}, hereafter. The quantitative description of the two magnetization dynamics must account both for different decays and for pseudo-solid spin echoes observed from the two relaxation parts.

3.1. Relaxation Functions. The expression of the relaxation function which has proved to be a suitable tool for describing quantitatively the effect of chain dynamics on NMR (including tha analysis of PSOSES) has been already established and reported elsewhere;[16] it is shortly recalled here. Considering that any relaxation function must be determined from a spin−spin interaction Δ and a characteristic correlation time, τ_s, the proton transverse relaxation is described using a spectrum of n_s relaxation modes reminiscent of the Rouse model spectrum and defined as

$$\tau_p^{-1} = \tau_s^{-1} \sin^2(\pi p/n_s) \qquad p = 1, 2, ..., n_s - 1 \qquad (2)$$

τ_s is a characteristic correlation time. It has been shown

that for each submolecule, the general expression of the magnetization $M_x(t,n_s)$ can be written as an exponential function of the second-order term of a cumulant expansion:

$$M_x(t,N) = \exp[-C(t,N)\,]\Phi_R(t) \quad (3)$$

with

$$C(t,N) = \Delta^2 \int_0^t dt_1 \int_0^{t_1} dt_2\, \Gamma(|t_1 - t_2|; n_s) \quad (4)$$

and

$$\Gamma(|t_1 - t_2|; n_s) = \left[\frac{1}{n_s}\sum_{P=1}^{n_s-1} \exp(-|t_1 - t_2|/\tau_s)\sin^2(\pi p/n_s)\right]^2 \quad (5)$$

Considering eq 5, it is seen that the spectrum involved in NMR properties consists of n_s^2 modes defined from

$$\tau_{p,q}^{-1} = \tau_s^{-1}(\sin^2(\pi p/n_s) + \sin^2(\pi q/n_s)) \qquad p, q = 1, 2, ..., n_s - 1 \quad (6)$$

Correspondingly, there is an equipartition Δ/n_s of the residual dipole−dipole coupling. Consequently, the motional averaging effect of each relaxation mode applies to the very weak coupling Δ/n_s and the relative contribution of each mode is $1/n_s^2$. At long times, the $C(t,N)$ function reads

$$C(t,N) = 1.35\Delta^2\tau_s t \quad (7)$$

corresponding to an exponential time function characterized by the rate $1/T_R = 1.35\Delta^2\tau_s$. Applying eqs 2−7 to the analysis of the parts I and II of relaxation curves, it will be shown that the residual dipole−dipole interactions $\Delta = \Delta_{II}$ for end-submolecules or $\Delta = \Delta_I$ for the remaining submolecules are invariant with respect to chain molecular weight variations and that numerical results are independent of the number of modes, n_s, provided n_s is greater than 15.

3.2. Pseudo-Solid Spin—Echoes. The residual dipole−dipole coupling confers a pseudo-solid behavior on the proton magnetization which is well detected from the formation of spin echoes specific to pure solid-state NMR too. In the case of a polymer melt, the slow time evolution of chain conformations affects this time reversal effect; for example, this effect cannot be observed from short chains ($M \leq 10^4$ for PB) because their random rotation is fast enough to fully average spin−spin interactions during the proton relaxation.[6] The expression describing PSOSES has been already reported for noninteracting proton pairs; however, attention was not focused on the numerical analysis of these echoes specific to long chains or to polymeric networks.[6] In accordance with the description of $M_x(t)$, the pseudo-solid spin echo $E_x(t, \tau; N)$, formed at $t = \tau$, has been shown to be expressed according to the function:

$$E_x(t; \tau; N) = \exp[-(2\,C(t,N) + 2C(t - t,N) - C(t,N))]\Phi_R(t) \quad (8)$$

As shown elsewhere for PEO,[11] the logarithmic derivative of $\Phi_R(t)$ at $t = \tau$ can be derived from the limiting value of the equation

$$\frac{1}{\Phi_R(t)}\frac{d\Phi_R(t=\tau)}{dt} = [E_x(t; \tau;N) + M_x(t,N) - 2M_x(t,N)\,]/[2(t - \tau)\,M_x(t,N)] \quad (9)$$

obtained for $t = \tau$;[16] expressions for $\Phi_R(t)$ will be given in the next section. Also, the derivative of $C(t; N)$ at $t = \tau$ can be derived from the limiting value of the equation

$$dC(t;N)/dt = [E_x(t; \tau;N) - M_x(t,N)]/[2(t - \tau)\,M_x(t,N)] \quad (10)$$

obtained for $t = \tau$. Furthermore, the difference $E_x(t; \tau; N) - M_x(t,N)$ has been shown to exhibit a maximum at a time $t_m(\tau)$ depending on τ; the limiting value of $1/t_m(\tau)$ for $\tau = 0$ is Δ.[6]

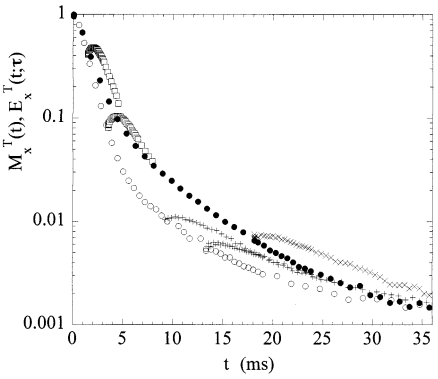

Figure 1. Proton transveres relaxation in polybutadiene: (●) $M = 67 \times 10^3$; (○) $M = 206 \times 10^3$. Pseudo-solid spin echoes formed from the part I relaxation (□) are well distinguised from those formed from the part II (+, ×).

4. Results and Discussion

It is not the purpose of this paper to recall all details about the procedure of numerical analysis of the proton transverse relaxation; semilogarithmic and $\ln(M_x(t))/t$ plots were used for determining exponential relaxation rates while relaxation curves and PSOSES were combined according to eqs 9 and 10 for estimating the residual dipole−dipole couplings. Typical relaxation curves and PSOSES observed from PB ($M = 67 \times 10^3$ and 206×10^3) at 300 K are shown in Figure 1; they are similar to relaxation curves recorded from PEO.[11] The slow relaxation of the proton magnetization (part II) associated with end-submolecules is well distinguished from the fast relaxation of the magnetization (part I) of protons attached to the remaining part of one chain. Also, in addition to their different relaxation time scales (about 20 and 4 ms, respectively), these two parts of the relaxation curves are distinguished from each other by observing the shapes of PSOSES. Echoes formed from the end-submolecule magnetization are flat whereas those formed from part I are well-shaped.

The analysis of relaxation curves starts from the characterization of the proton magnetization associated with end-submolecules.

4.1. End-Submolecules. At long times ($t > 10$ ms), the part I relaxation is negligible and the part II relaxation was easily characterized from the molecular weight dependent pattern of two species of curves: relaxation and PSOSES; the description was strongly reinforced by analyzing five PSOSES for each molecular

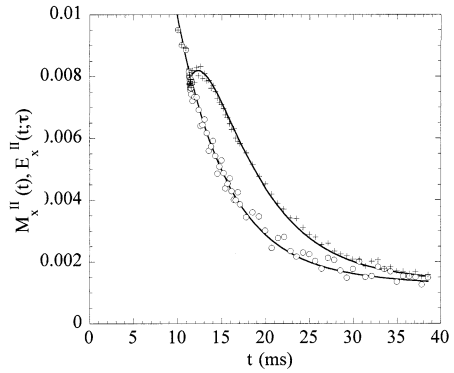

Figure 2. Relaxation curve (○) and pseudo-solid echo (+) computed from eqs 2−5 and 8 with $A_{II} = 0.035$ and numerical values independent of chain molecular weight: $\Delta_{II} = 260$ rad·s^{-1}, $1/T_2^{II} = 43$ s^{-1}, and $\tau_s^{II} = 1.6$ ms ($M = 206 \times 10^3$).

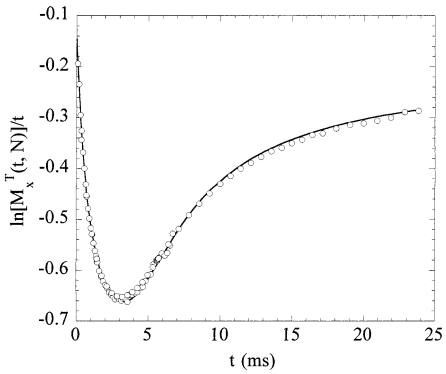

Figure 3. $\ln[M_x^T(t,M)]/t$ plot of the proton transverse relaxation curve recorded from molten polybutadiene (○) at 298 K (116×10^5). Illustration of the numerical fit (continuous curve) calculated according to eqs 2−5, 11, and 13, using the following numerical values independent of chain molecular weight: $\Delta_I = 1250$ rad·s^{-1}, $1/T_2^I = 140$ s^{-1}; $\Delta_{II} = 260$ rad·s^{-1}, $1/T_2^{II} = 43$ s^{-1}, and $\tau_s^{II} = 1.6$ ms; $\tau_s^I = 0.39$ ms and $A_{II} = 0.058$.

weight within the range $41 \times 10^3 \leq M \leq 375 \times 10^3$. Considering eqs 2−5 and 8 the part II relaxation function was written as

$$M_x^{II}(t,N_{II}) = A_{II} \exp[-C_{II}(t,N_{II})]\Phi_R^{II}(t) \qquad (11)$$

while the PSOSE was expressed as

$$E_x^{II}(t;\tau;N_{II}) = A_{II} \exp[-(2C_{II}(\tau;N_{II}) + 2C_{II}(t-\tau;N_{II}) - C_{II}(t;N_{II})]\,\Phi_R^{II}(t) \qquad (12)$$

At long times ($t > 10$ ms) $M_x^{II}(t,N_{II})$ was found to behave as an exponential time function characterized by a relaxation rate equal to 189 s^{-1}; consequently, in accordance with eqs 7 and 11, $\Phi_R^{II}(t)$ was determined from semilogarithmic plots as an exponential function characterized by the rate $1/T_2^{II}$. The best fits were obtained by computing the pattern of $M_x^{II}(t,N_{II})$ relaxation curves and $E_x^{II}(t;\tau;N_{II})$ echoes, from a single value for $1/T_2^{II} = 43 \pm 1$ s^{-1} and a single value for the residual dipole−dipole coupling $\Delta_{II} = 260 \pm 5$ rad·s^{-1} while the correlation time τ_s^{II} equal to $(1.6 \pm 0.05) \times 10^{-3}$ s was derived from the expression of $1/T_R$ (eq 7) with $1/T_R = 189$ s^{-1} − $1/T_2^{II}$. Furthermore, eq 10, independent both of $\Phi_R^{II}(t)$ and of the amplitude A_{II}, was used to confirm numerical values of Δ_{II} and τ_s^{II}. The fit corresponding to a relaxation curve and to a PSOSE formed at $\tau = 11.45$ ms ($M = 206 \times 10^3$) is illustrated in Figure 2. It is worth noting that the molecular weight dependence of $M_x^{II}(t,N_{II})$ appeared only through the amplitude A_{II} adjusted to the best fits and used for determining the number N_{II} of monomeric units in one end-submolecule. A_{II} was the only molecular weight dependent quantity within the range 41×10^3 $M \leq 375 \leq 10^3$. For the amplitude A_{II} of part II magnetization, the product $A_{II}M/2 = M_{End}(T)$ has been already found to be hardly dependent on chain length at a given temperature ($A_{II}M/2 = 760M^{0.1}$ with M). $M_{End}(T) = (3.3 \pm 0.15) \times 10^3$ is considered as the mean molecular weight of one end-submolecule, at 300 K and the mean number of monomeric units forming one end-submolecule is $N_{II} = 61 \pm 3$. Finally, the numerical simulation of PSOSES required the number of modes, n_s, be equal to or higher than 14; for $n_s > 14$ the fit was independent of n_s. In previously reported works $M_x^{II}(t)$ was roughly described as an exponential time function; however, considering eqs 2, 7 and 8, it is worth noting that no PSOSE can be formed when the relaxation curve is expressed as a simple exponential time function. For NMR, end-submolecules are considered as dynamic probes which behave nearly like free short chains ($1/T_2 \approx 20$ s^{-1}).[6]

4.2. Inner Submolecules. Similarly, the part I magnetization, $M_x^I(t,N)$, was analyzed also using eqs 2−5; $M_x^I(t,N)$ was expressed as

$$M_x^I(t,N) = (1-A_{II}) \exp[-C_I(t,n_s)]\exp(-t/T_2^I) \qquad (13)$$

The total relaxation function $M_x^T(t,N)$ was expressed from eqs 11 and 13 as the sum of $M_x^I(t,N)$ and $M_x^{II}(t,N)$. The plot of the ratio $\ln[M_x^T(t,N)]/t$ exhibits a minimum which is a suitable and sharp criterion for fitting experimental relaxation curves; a typical fit is shown in Figure 3 for the relaxation curve recorded from a 116×10^5 PB sample, at 298 K. $\Phi_R^I(t)$ was found to be an exponential function with a relaxation rate $1/T_2^I$ equal to 140 s^{-1}. The $C_I(t,N)$ function was computed from the residual dipole−dipole coupling Δ_I equal to 1250 ± 10 rad·s^{-1}; as noted in section 3.2, Δ_I was derived from the measured limiting value $1/t_m(0)$: $\Delta_I = 1/t_m(0) - \Delta_{II}$. The pattern of relaxation curves $M_x^I(t,N)$ recorded as a function of molecular weight was described from two adjustable parameters: $1/T_2^I$ and the correlation time τ_s^I; the amplitude was set equal to $1 - A_{II}$. $1/T_2^I$ and Δ_I were found to be independent of chain molecular weight within the range $41 \times 10^3 \leq M \leq 375 \times 10^3$ while the correlation time τ_s^I was shown to exhibit a slight molecular weight dependence represented in Figure 4A. Because the part II relaxation has been roughly described in previous works, the numerical analysis has not been accurate enough to reveal the molecular weight dependence of τ_s^I, suggesting only a slight molecular weight dependence for the product $\Delta_I\tau_s^I$.

Intersection Property of $M_x^I(t;N)$. The striking molecular weight dependence of τ_s^I can be given a direct evidence by considering the property of intersection of $M_x^I(t,N)$ relaxation curves. This property has been also well observed from PEO but has not been given any theoretical analysis, yet;[6,14] it is illustrated here, in Figure 5, from $M_x^I(t,N)$ relaxation curves obtained from the best $M_x^T(t,N)$ fits. Let $P_i = 0.56$ denote

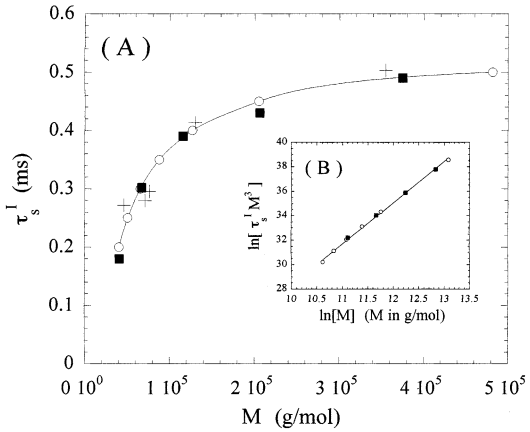

Figure 4. (A) Experimental (■) and theoretical (from eq 14, ○) molecular weight dependence of the correlation time τ_s^I; (+) melt viscosity divided by M^3 from data reported in ref 17. (B) Experimental (■) and theoretical (○) molecular weight dependence of the product $\tau_s^I M^3$.

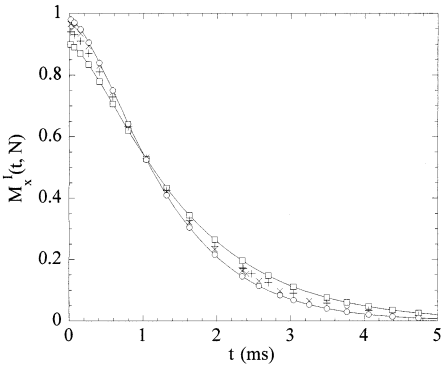

Figure 5. Illustration of the intersection property of $M_x^I(t,M)$ curves obtained from the best fits, at 328 K: (□) 67×10^3; (+) 116×10^3; (×) 206×10^3; (○) 375×10^3.

the amplitude of $M_x^I(t,N)$ at the intersection time $t_i^I = 0.964$ ms, the intersection property implies the following equation derived from eq 13

$$C_I(u_i; n_s)/u_i^2 + 1/t_i^I T_2^I = [-\ln(P_i) + \ln(1-A_{II})]/(t_i^I)^2 \quad (14)$$

with $u_i = t_i^I/\tau_s^I$; considering the amplitude A_{II} as a variable, τ_s^I had no explicit expression and was calculated as a numerical solution of eq 14. The exact intersection of $M_x^I(t,N)$ curves requires the segmental correlation time τ_s^I be molecular weight dependent according to the theoretical curve shown in Figure 4A; the theoretical product $M^3\tau_s^I$ was found to exhibit an apparent power law $M^{3.31}$ over the molecular weight range: 40×10^3 to 480×10^3 (Figure 4B).

Pseudo-Solid Spin—Echoes. Considering each fitted $M_x^T(t,N)$ relaxation curve, any PSOSE could be computed from the following equations

$$E_x^T(t; \tau) = E_x^I(t; \tau) + E_x^{II}(t; \tau) \quad (15)$$

with

$$E_x^I(t; \tau) = \exp[-(2C_I(t,n_s) + 2C_I(t-\tau, n_s) - C_I(t,n_s)) + \kappa\tau(t-\tau)] \exp(-t/T_2^I) \quad (16)$$

The parameter $\kappa = 0.11$ ms^{-2} was introduced empirically to account for the dipolar interaction between $-(CH_2)$ and $-(CH{=}CH)-$ proton pairs (κ has negligible effects on echoes formed within the range $0 \le \tau \le 1$ ms); the very good agreement between theoretical echoes and experimental ones recorded from a 116×10^3 PB sample at 298 K is illustrated in Figure 6. It may be worth emphasizing that the description of PSOSES observed in PEO does not necessitate the introduction of the parameter interaction κ since there is only one species of proton pairs.

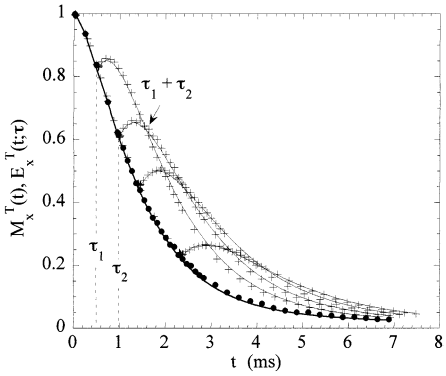

Figure 6. Illustration of pseudo-solid spin echoes (continuous lines) calculated according to eqs 8, 15, and 16 ($M = 116 \times 10^5$, $\Delta_I = 1250$ rad·s^{-1}, $\tau_s^I Z = 0.39$ ms, $1/T_2{}^I = 140$ s^{-1}, $1/T_2^{II} = 43$ s^{-1}, $A_{II} = 260$ rad·s^{-1}, $\tau_s^{II} = 1.6$ ms, $A_{II} = 0.058$, and $\kappa = 0.12$ ms^{-2}) and illustration of the intersection property of pseudo-solid spin echoes

Intersection Property of any Two PSOSES. Let us consider two echoes $E_x^T(t; \tau_1)$ and $E_x^T(t; \tau_2)$ formed at times τ_1 and τ_2 , respectively; it is easily seen from eqs 12, 15, and 16 that their intersection must occur at $t = \tau_1 + \tau_2$. In this work, it is shown that the property of PSOSE intersection that is well observed for pure residual spin−spin interactions in permanent networks extends to temporary networks as shown from experimental echoes drawn in Figure 6.

It is worth noting that the good agreement between fits and observed PSOSES reinforces the reliability of the proton relaxation description which is not considered as a simple numerical adjustment.

The total relaxation function $M_x^T(t,N)$ accounts both for the property of intersection of $M_x^I(t,n_s)$ and for characteristic properties of recorded pseudo-solid echoes.

4.3. Discussion. For the polybutadiene self-diffusion, the molecular weight crossover between the Rouse regime and the reptation one is $M_D = 31.7 \times 10^3$. For molecular weights higher than M_D, the interpretation of the proton transverse relaxation observed in PB within the range $41 \times 10^3 \le M \le 375 \times 10^3$ implies the description of a pattern of relaxation curves which consist of two parts representing two independent magnetizations; each part exhibits two species of curves: relaxation and PSOSES. The underlying hypothesis about the interpretation of the relaxation is the existence of submolecules originating from the effect of the chain entanglement interaction: end-submolecules and inner ones. However, for $M \le 40 \times 10^3$, the magnetization dynamics of these two types of submolecules are not easily distinguished from each other; this result illustrates the existence of a crossover which spreads over the range $(31.7-40) \times 10^3$ for the transverse magnetization. The description of 10 relaxation functions and more than 30 PSOSES recorded from five samples with different molecular weights corresponds

to the detection of four types of motions and is inevitably based on the determination of four parameters adjusted to the best fits and three quantities determined directly from relaxation plots without any adjustment. Two relaxation rates were associated with fast but nonisotropic monomeric motions which occur within end-submolecules or within inner ones while two spin−spin interactions and two correlation time were associated with internal rearrangements of end-submolecules and inner submolecules. The correlation time τ_s^I associated with inner submolecules and the relative end-submolecule amplitude A_{II} (seventh quantity) were the only chain length dependent quantities. The variation of τ_s^I must start from from the crossover molecular weight M_d ($\tau_s^I \approx 0.2$ ms); Figure 4A shows that it levels off for molecular weights higher than 415×10^3 while the product $M^3\tau_s^I$ exhibits a $M^{3.31}$ power law within this intermediate range (Figure 4B). Considering the polybutadiene melt viscosity η_0 measured within the range 50×10^3 to 400×10^3, it is worth emphasizing that Colby et al. have already reported a similar transient regime for the ratio η_0/M^3 corresponding to an apparent power law $M^{0.41}$.[17] Considering one inner submolecule comprised of N_I monomeric units, it is supposed that the correlation time $\tau_s^I \approx 0.4$ ms may be expressed as a function of N_I and of an effective segmental friction coefficient ζ_s

$$\tau_s^I = \frac{C_\infty b^2}{3kT}\,\zeta_s N_I \qquad (17)$$

with $C_\infty b^2 = 47.3$ Å^2 per monomeric unit;[18] a rough estimate of $\zeta_s \approx 1.7 \times 10^{-7}$ kg·s^{-1} is obtained by assuming that $N_I \approx 61$ monomeric units. The order of magnitude of this estimate shows that τ_s^I must be assigned to a long chain segment rather than to a few monomeric units; consequently, it is supposed that its molecular weight dependence characterizes a segmental friction effect rather than a local one. This work shows that the macroscopic dynamics behavior reflected by the viscosity originates actually from a semilocal property.

The number $N_{II} = 61$ of monomeric units forming one end-submolecule has been shown to be closely associated with the monomeric friction coefficient ζ_0 measured from short chain diffusion: the ratio $\zeta_0 N_{II}^2/kT$ is nearly constant over the temperature range 298−358 K ($N_{II} \approx$ 146 at 358 K, $\Delta_{II} = 150$ rad·s^{-1} and $\tau_s^{II} = 2.45$ ms while $\zeta_0 = 2 \times 10^{-10}$ kg·s^{-1}).[6] The increase of the segmental size of end-submolecules detected when the temperature is raised is still unexplained. The limiting value of A_{II} corresponding to M_D is 0.21.

The strength of the dipole−dipole interaction $|\mathbf{H}_D| = I(I+1)\gamma^2 h/2\pi r^3$, equal to 10^5 rad·s^{-1} within a −(CH$_2$) proton pair with $I = {}^1/_2$ and $r = 1.78$ Å (0.39×10^5 rad·s^{-1} for a −(CH═CH)− proton pair with $r = 2.43$ Å), was chosen as a reference. It is now well established that the reduction factor of the dipole−dipole coupling within one proton pair attached to a fluctuating Gaussian segment comprised of n monomeric units can be simply expressed as the ratio β/n; the numerical value of β accounts both for the chain stiffness and for the quantum average. The residual dipole−dipole coupling Δ_{II} associated with end-submolecules was written as $\Delta_{II} = \beta_{II}|\mathbf{H}_D|/N_{II}$, with $\beta_{II} = 0.16$.

The observation of characteristic NMR properties predicted from the model proves that $M_x^T(t,N)$ is a reliable tool for probing the experimental molecular weight dependence of the segmental correlation time τ_s^I. This treatment does not apply to low molecular weight PB ($M \leq 40 \times 10^3$). Investigations into NMR properties previously reported about poly(ethylene oxide) and PB were not focused on the quantitative description of pseudo-solid spin echoes and the property of intersection of $M_x^I(t,N)$ curves was never applied to the characterization of the molecular weight dependence of the segmental correlation time τ_s^I.[6]

Finally, the relaxation rates $1/T_2^I$ and $1/T_2^{II}$, reflecting fast and nonisotropic motions of monomeric units, were roughly expressed as the product of a mean square dipole−dipole interaction (10^{10} (rad·s^{-1})^2) and a correlation time equal to 0.43×10^{-8} and to 1.4×10^{-8} s for monomeric units attached to end-submolecules or to inner submolecules, respectively.

5. Conclusion

It is shown throughout this work that the interpretation of proton magnetic relaxation in molten PB is quantitative and in very good agreement with experimental results; intrinsic properties of chain dynamics in a melt set the time scale of NMR investigations around 1 ms. In addition to the rough characterization of fast but nonisotropic motions of monomeric units, this study provides two unambiguous main features. First, in agreement with the reptation model, it gives a clear evidence for the existence of two qualitatively distinct random motions affecting two different parts of one chain: on one hand, end-chain segments, represented by about 61 monomeric units at room temperature, behave nearly like free short chains, and on the other hand, the inner part of one chain is characterized by much less isotropic motions of monomeric units. Second, the displacement of the inner part of one chain is characterized by a molecular weight dependent semilocal correlation time determined around 0.4 ms. Implying an effective segmental friction effect varying as a function of molecular weight, this property observed as a reliable new result leads to exponents in agrement with 3.3 ± 0.1 and 2.3 ± 0.1 exponents determined from viscosity and chain diffusion, respectively. Furthermore, the experimental reconciliation of the molecular weight dependence of diffusion and zero-shear rate viscosity has been carefully analyzed by Lodge for solutions and melts;[5] the reconciliation implies a molecular weight exponent for the terminal relaxation time of reptation, T_r, equal to 3.3 ± 0.1 in agreement with reptation simulations. Several approaches attempting to explain the exponent of viscosity have been proposed, considering constraint release and contour length fluctuations effects[19−21] while the two-armed star model provided a power law for the low frequency dependence of the loss modulus in agreement with experiment.[22] Long range chain properties are involved in those theoretical approaches; it was the intent of this work to show that the apparent 0.3 value added to exponents calculated from the reptation model was experimentally detected not only during the terminal part of chain relaxation (viscosity, diffusion) but also during the considerably shorter 1 ms time scale. It is an elementary effect which in turn governs the dynamics of a whole chain. In agreement with recent numerical simulations, the additional exponent does not apply above a molecular weight threshold, about equal to 500×10^3 for polybutadiene at room temperature.

Keeping the tube concept in mind, it is considered here that the roughness experienced by one so-called primitive chain depends on the tube length. This effect may be due to tube erosion related to the finite lifetime of strong lateral constraints exerted on one chain during its back and forth translational motion. Considering one chain, this erosion may be induced by the random retraction of all end-submolecules embedded in this chain and unambiguously detected from their magnetization dynamics. The challenge to the chain dynamics description as shifted toward about 1 ms results from the new insight provided by low resolution NMR investigations.

Acknowledgment. Financial support from du Pont de Nemours (Europe) is gratefully acknowledged.

References and Notes

(1) Ferry, J. D. *Viscoelastic Properties of Polymers*; Wiley: New York, 1980.
(2) De Gennes, P. G. *J. Chem. Phys.* **1971**, *53*, 572.
(3) Curtiss, C. F.; Bird, R. B. *J. Chem. Phys.* **1981**, *74*, 2016.
(4) Tao, H.; Lodge, T. P.; von Meerwall, E. D. *Macromolecules* **2000**, *33*, 1747.
(5) Lodge, T. P. *Phys. Rev. Lett.* **1999**, *83*, 3218.
(6) Guillermo, A.; Cohen Addad J. P. *J. Chem. Phys.* **2002**, *116*, 3141.
(7) Kreer, T.; Baschnagel, J.; Mûller, M.; Binder, K. *Macromolecules* **2001**, *34*, 1105.
(8) Masubuchi, Y.; Takimoto, Jun-Ichi; Koyama, K.; Ianniruberto, G.; Marrucci, G *J. Chem. Phys.* **2001**, *115*, 4387.
(9) Graessley, W. W. *Adv. Polym. Sci.* **1974**, *16*, 1.
(10) Graessley, W. W.; Edwards, S. F. *Polymer* **1981**, *22*, 1329.
(11) Cohen Addad, J. P.; Guillermo, A. *J. Chem. Phys.* **1999**, *111*, 7131.
(12) Cohen Addad, J. P.; Guillermo, A. *Phys. Rev. Lett.* **2000**, *85*, 3432.
(13) Guillermo, A.; Cohen Addad J. P.; Bytchenkoff, D. *J. Chem. Phys.* **2000**, *113*, 5098.
(14) Kimmich, R.; Köpf, M.; Callaghan, P. *J. Polym. Sci., Polym. Phys. Ed.* **1991**, *29*, 1025.
(15) Klein, P. G.; Adams, C. H.; Brereton, M. G.; Ries, M. E.; Nicholson, T. M.; Hutchings, L. R.; Richards, R. W. *Macromolecules* **1998**, *31*, 8871.
(16) Cohen Addad, J. P. NMR and Fractal Properties of Polymeric Liquids and Gels. In *Progress in NMR Spectroscopy*; Emsley, J. W., Feeney, J., Sutcliffe, L. H., Eds.; Pergamon Press: Oxford, England, 1993; pp 51−89.
(17) Colby, R. H.; Fetters, L. J.; Graessley, W. W. *Macromolecules* **1987**, *20*, 2226.
(18) Fetters, L. J.; Lohse, D. J.; Richter, D.; Witten, T. A.; Zirkel, A. *Macromolecules* **1994**, *27*, 4639.
(19) Doi M.; Edwards, S. F. *The Theory of Polymer Dynamics*; Clarendon Press: Oxford, England, 1988.
(20) Lodge, T. P.; Rotstein, N. A.; Prager, S. *Adv. Chem. Phys.* **1990**, *79*, 1.
(21) Likhtman, A. E.; McLeish, T. C. B. *Macromolecules* **2002**, *35*, 6332.
(22) Milner, S. T.; McLeish, T. C. B. *Phys. Rev. Lett.* **1998**, *81*, 725.

MA021567Y